Carrier Multiplication in Quantum Dots within the Framework of Two Competing Energy Relaxation Mechanisms

ARTICLE *in* JOURNAL OF PHYSICAL CHEMISTRY LETTERS · JUNE 2013

Impact Factor: 7.46 · DOI: 10.1021/jz4004334

6 AUTHORS, INCLUDING:

Wan Ki Bae
Korea Institute of Science and Technology
54 PUBLICATIONS **1,534** CITATIONS
SEE PROFILE

Weonkyu Koh
Samsung Advanced Institute of Technology
23 PUBLICATIONS **704** CITATIONS
SEE PROFILE

THE JOURNAL OF PHYSICAL CHEMISTRY Letters

Perspective

pubs.acs.org/JPCL

Carrier Multiplication in Quantum Dots within the Framework of Two Competing Energy Relaxation Mechanisms

John T. Stewart, Lazaro A. Padilha, Wan Ki Bae, Weon-Kyu Koh, Jeffrey M. Pietryga, and Victor I. Klimov*

Center for Advanced Solar Photophysics, C-PCS, Chemistry Division, Los Alamos National Laboratory, Los Alamos, New Mexico 87545, United States

ABSTRACT: The realization of high-yield, low-threshold carrier multiplication (CM) in semiconductor quantum dots (QDs) is a promising step toward third-generation photovoltaics (PV). Recent studies of QD solar cells have shown that CM can indeed produce greater-than-unity quantum efficiencies in photon-to-charge-carrier conversion, establishing the relevance of this process to practical PV technologies. While being appreciable, the reported CM yields are still not high enough for a significant increase in the power conversion efficiency over traditional bulk materials. At present, the design of nanomaterials with improved CM is hindered by a poor understanding of the mechanism underlying this process. Here, we present a possible solution to this problem by introducing a model that treats CM as a competition between impact-ionization-like scattering and non-CM energy losses. Importantly, it allows for evaluation of expected CM yields from fairly straightforward measurements of Auger recombination (inverse of CM) and near-band-edge carrier cooling. The validation of this model via a comparative CM study of PbTe, PbSe, and PbS QDs suggests that it indeed represents a *predictive* capability, which might help in the development of nanomaterials with improved CM performance.

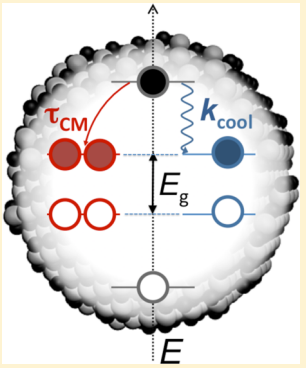

Carrier multiplication (CM) is a process whereby multiple electron−hole (e−h) pairs (multiexcitons) are generated via absorption of a single photon.[1] This process is distinct from a more common mechanism whereby multiexcitons are produced at high pump intensities via sequential absorption of multiple photons.[2,3] Ideally, CM yields are limited just by energy conservation. The dependence of the corresponding quantum efficiency (QE) of photon-to-exciton conversion on incident photon energy ($\hbar\omega$) is described by a staircase function, in which each increment in $\hbar\omega$ by the band gap (E_g) results in a new e−h pair (Figure 1a; blue solid line). In bulk semiconductors, CM occurs via impact ionization, where a valence band electron is promoted to the conduction band via a collision with a high-energy charge carrier.[4] In this traditional picture, the efficiency of CM is set by the competition between impact ionization and phonon emission. In addition to conserving energy, impact ionization conserves translational momentum, which together with phonon-assisted energy losses reduces the CM yields below the ideal values (Figure 1a; red dashed line).

Quantum-confined semiconductor nanocrystals, or quantum dots (QDs), have been expected to exhibit enhanced CM due to the discrete structure of their electronic states, which can slow phonon emission through a "phonon bottleneck"[5] and can also lead to relaxation of translational momentum conservation,[6] lowering the spectral threshold for this effect. The first spectroscopic observation of efficient CM in PbSe QDs[7] stimulated fervent activity in this area, including spectroscopic studies of multiexciton generation[8−15] and multiexciton extraction/dissociation,[16,17] the development of practical devices exploiting CM,[18−20] as well as theoretical modeling of CM-based solar cells.[21−23] These studies have resulted in significant recent progress in the understanding of CM and related processes. However, the published reports indicate that even in materials with the strongest CM performance, such as PbSe nanorods[24−26] and Si QDs,[27−29] the QE of photon-to-exciton conversion within the solar photovoltaic (PV)-relevant spectral range is still not sufficiently high to appreciably increase power conversion efficiency of practical devices.[21,22,30] This assessment highlights the need for new nanostructures tailored to optimize CM for energies relevant to solar energy conversion. One complication in the development of such materials is the lack of an established theory for treating this process in quantum-confined nanocrystals. For example, in addition to traditional impact ionization models,[31−36] there have been a number of other approaches that rely on QD-specific physics, including quantum mechanical superposition of single-exciton and biexciton states,[37,38] direct photogeneration,[39−43] and "quantum cutting" of an incident photon to produce two excitons in adjacent NCs.[44,45]

To facilitate ongoing experimental efforts in the search for more efficient CM materials, here, we propose an *experiment-inspired* phenomenological model of CM, which treats this process in terms of a competition between impact-ionization-like scattering and non-CM energy losses. Using this model, we can evaluate the expected CM yields of QDs from physical properties of a parental bulk solid and/or fairly straightforward

Received: February 26, 2013
Accepted: May 30, 2013

   dx.doi.org/10.1021/jz4004334 | *J. Phys. Chem. Lett.* 2013, 4, 2061−2068

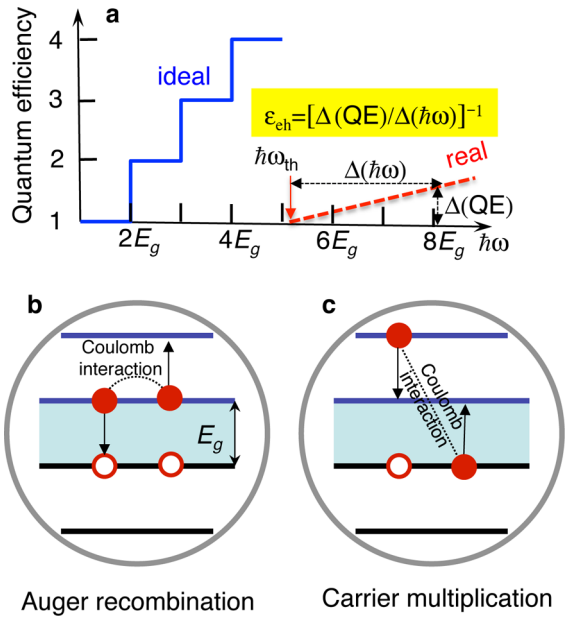

Figure 1. CM and the inverse process of Auger recombination. (a) The ideal, staircase-like QE of photon-to-exciton conversion is limited only by energy conservation (blue solid line). Due to additional restrictions associated with translational momentum conservation and phonon-related energy losses, the QEs observed for bulk materials (red dashed line) are lower than those in the ideal case. The e−h pair creation energy (ε_{eh}) is defined by the inverse of the slope of the dependence of QE on the photon energy ($\hbar\omega$) above the spectroscopic onset of CM ($\hbar\omega_{th}$). (b) In the course of Auger decay of a biexciton, the energy released during recombination of one of the excitons is transferred to a third carrier (an electron in the case shown in the figure). (c) During CM, the energy of a hot carrier (an electron in the figure) is relaxed by exciting a valence band electron across the energy gap (E_g), which results in a new exciton. This process can be pictured as the inverse of Auger decay and vice versa.

measurements of Auger recombination and near-band-edge carrier cooling. We validate this model by applying it to our measurements of PbTe, PbSe, and PbS QDs, for which it correctly describes the relative CM efficiencies among all three compounds, suggesting that this phenomenological description indeed represents a useful tool in the search for more efficient CM materials.

At the center of our model and our measurements is the e−h pair creation energy (ε_{eh}), a key parameter that directly accounts for the competition between impact-ionization-like events producing new excitons and non-CM intraband relaxation.

At the center of our model and our measurements is the e−h pair creation energy (ε_{eh}), a key parameter that directly accounts for the competition between impact-ionization-like events producing new excitons and non-CM intraband relaxation. This quantity can be defined as the increment in the energy of an incident photon required to produce a new exciton at energies above the spectroscopic threshold of CM ($\hbar\omega_{th}$); see Figure 1a. In the case of optical studies, ε_{eh} is determined from measurements of QE or the CM yield (η = QE − 1) as a function of excitation energy $\varepsilon_{eh} = [d(QE)/d(\hbar\omega)]^{-1} = [d\eta/d(\hbar\omega)]^{-1}$, or more simply stated, ε_{eh} is the inverse of the slope of the QE versus $\hbar\omega$ dependence at energies above $\hbar\omega_{th}$.

In order to resolve ε_{eh} into its constituent mechanisms (that is, the processes responsible for CM and non-CM energy losses), we start with an analysis of biexciton Auger lifetimes (τ_{2A}). During biexciton Auger decay, one exciton recombines by transferring its energy to the second exciton, which is re-excited to a higher-energy "hot" state (Figure 1b). This is exactly the inverse of CM, and therefore, both processes are described by the same Coulomb matrix element, at least in the situation when CM occurs near the energy-conservation-defined threshold, as shown in Figure 1c. However, even in this case, due to the involvement of different densities of final states (single exciton for Auger decay and biexcitons for CM), τ_{2A} is not exactly equal but only proportional to the characteristic time of an individual CM event (τ_{CM}). Furthermore, as the time scale of intraband relaxation is much shorter than the Auger decay time, Auger recombination occurs primarily with participation of carriers in relaxed band edge states. On the other hand, CM involves "hot" carriers with energies that can be well above the CM "energetic" threshold, which leads to further distinction between τ_{CM} and τ_{2A}. Nonetheless, we speculate that while the absolute value of τ_{2A} can be considerably different from the value of τ_{CM}, the Auger lifetimes can still be used as a *surrogate* for τ_{CM} for the purpose of comparing CM time constants between QDs of different compounds.[46]

In Figure 2a, we compare the τ_{2A} lifetimes measured for PbTe (open blue symbols), PbSe (red symbols), and PbS (black symbols) QDs plotted as a function of confinement energy ($E_c = E_g - E_{g,0}$, where $E_{g,0}$ is the respective bulk semiconductor band gap). The Auger time constants are very similar for these three types of QDs, which suggests the similarity of the τ_{CM} values and further might be considered as an indication of similar CM performance. However, as we show below, direct measurements of CM contradict these expectations, indicating a considerable difference in the multiexciton yields for the QDs of these three compounds.

The CM efficiencies were measured at 3.1 eV using transient absorption (TA)[7] and two distinct transient photoluminescence (PL) experiments, one utilizing PL upconversion (uPL)[47] and the other a superconducting nanowire single-photon detector (SSPD).[24] The methods used to extract the CM efficiency from TA and PL time traces rely on the detection of the Auger decay signatures of multiexcitons[48] and are based on the evaluation of the amplitude of the early-time multiexciton signal (a) versus the late-time single-exciton background (b) (see Figure 2b).[7,47,49] To mitigate the distortion of CM signals due to photocharging, the samples were vigorously stirred during the measurements.[47,49−51] Further, to avoid fast initial transients unrelated to Auger decay, we only study well-passivated samples that do not show significant surface trapping and display "flat" TA and PL dynamics on a few nanosecond time scale when stirred and excited below the CM threshold at low pump fluence ($\langle N_0 \rangle \ll 1$; $\langle N_0 \rangle$ is the average number of photons absorbed per QD per pulse).

Examples of TA traces that illustrate a significant difference in CM yields between QDs of PbS, PbSe, and PbTe are

dx.doi.org/10.1021/jz4004334 | J. Phys. Chem. Lett. 2013, 4, 2061−2068

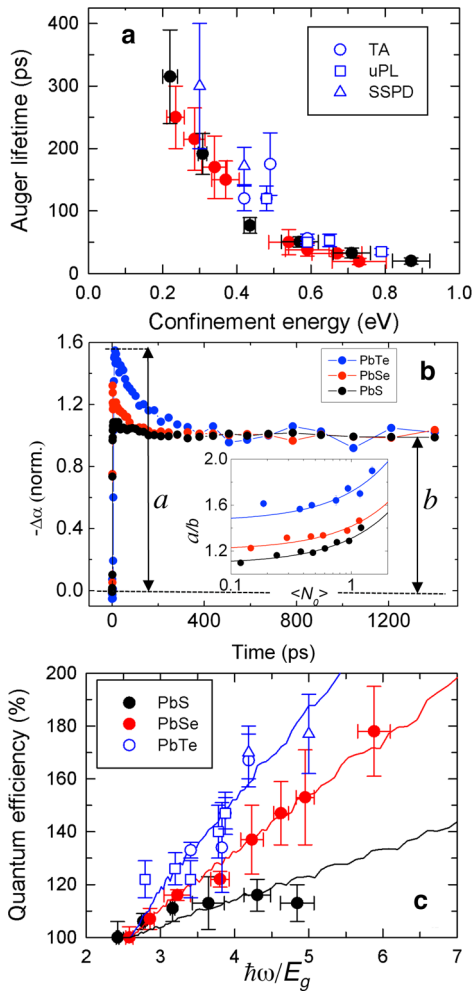

Figure 2. Measurements of Auger lifetimes and CM yields. (a) Biexciton Auger lifetimes are shown for differently sized PbS (solid black circles), PbSe (solid red circles), and PbTe (open blue symbols) QDs as a function of confinement energy. These data were obtained by monitoring pump-power-dependent QD population decay with three spectroscopic techniques, transient absorption (TA), time-resolved PL via femtosecond PL up-conversion (uPL), and time-resolved PL via time-correlated single-photon counting using a superconducting nanowire single-photon detector (SSPD); the exact technique used to obtain a specific data point is indicated explicitly for PbTe QDs in the figure legend (all data were collected using excitation at 1.5 eV with 100−300 fs pulses). A close correspondence between Auger lifetimes for QDs of all three compounds along with similar electronic structures suggests a similarity in the CM time constants. (b) TA traces for QDs of PbS (black), PbSe (red), and PbTe (blue) QDs; the samples have approximately the same band gap (0.83 eV for PbS, 0.8 eV for PbSe, and 0.8 eV PbTe QDs). In these experiments, we monitor the decay of the band edge 1S bleach ($\Delta\alpha$) following excitation with low-intensity ($\langle N_0\rangle$ of ca. 0.15), ~100 fs pulses at 3.1 eV. The recorded traces exhibit a fast initial component due to Auger decay of biexcitons generated primarily via CM. The difference in the amplitude of this component between QDs of different compounds indicates different CM efficiencies, with the highest CM yield observed in the PbTe QDs and the lowest in the PbS QDs. The CM QE is quantified from the extrapolation of the linear fit to the measured a/b ratio as a function of $\langle N_0\rangle$ to zero fluence (inset). (c) The summary of QE measurements for PbS, PbSe, and PbTe QDs as a function of photon energy normalized by E_g; these data were obtained for differently sized QDs (that is, different E_g) using excitation at a fixed photon energy of 3.1 eV. Jagged lines are a Monte Carlo modeling of CM yields, as described in the text.

displayed in Figure 2b. The traces are for samples of approximately the same band gap (0.83 eV for PbS, 0.8 eV for PbSe, and 0.8 eV for PbTe) that are excited with similar fluences ($\langle N_0\rangle$ of ca. 0.15). The inset shows the a/b ratio extracted from each of these samples (symbols) as a function of fluence. The a/b ratios are fit to a linear dependence (lines), and the QE of photon-to-exciton conversion is derived from the extrapolation of this fit to zero fluence. These data clearly demonstrate a progressive increase of the CM yield from PbS to PbSe and then to PbTe QDs. The same trend is also seen in the measurements of QDs with other band gaps, as demonstrated by the large collection of CM data in Figure 2c. From the linear fit to the measured data, we find that the E_g-normalized ε_{eh} increases from ~$2.8E_g$ in PbTe QDs to ~$4.3E_g$ in PbSe QDs and then to ~$12.5E_g$ in PbS QDs. Interestingly, this pronounced difference is observed despite the similarity in the τ_{CM} time constants expected based on Auger decay studies. This observation highlights the importance of considering the effect of energy loss channels competing with CM events.

The pronounced difference in ε_{eh} is observed despite the similarity in the τ_{CM} time constants expected based on Auger decay studies. This observation highlights the importance of considering the effect of energy loss channels competing with CM events.

To quantify the effect of non-CM energy relaxation, we consider the situation where the excitation energy is just above $\hbar\omega_{th}$. In this limit, the relaxation time (T) of a hot carrier from its original state (energy E_i; i = e or h for the electron and the hole, respectively) to the state that constitutes the CM threshold (energy $E_{i,th}$) is short compared to τ_{CM}. In this case, $\eta = T/\tau_{CM}$ or $\eta_i = (E_i - E_{i,th})/(k_{cool}\tau_{CM})$, if T is expressed in terms of a parameter, k_{cool}, that represents the rate of non-CM energy loss (this quantity is measured in units of, e.g., eV per ps). As optical excitation produces e−h pairs, the total CM yield is the sum of e−h pair producing events initiated by both a hot electron and a hot hole $\eta = \eta_e + \eta_h$. Assuming that τ_{CM}, k_{cool}, and $E_{i,th}$ are similar for electrons and holes (a reasonable assumption for Pb chalcogenides that have mirror-symmetric conduction and valence bands) and expressing $(\hbar\omega - \hbar\omega_{th})$ as $\sum_{i=e,h}(E_i - E_{i,th})$, we obtain $\eta = (\hbar\omega - \hbar\omega_{th})/(k_{cool}\tau_{CM})$, which further yields the following expression for the e−h pair creation energy $\varepsilon_{eh} = d(\hbar\omega)/d\eta = k_{cool}\tau_{CM}$. This expression indicates that this quantity indeed captures the competition between CM and non-CM relaxation processes.

To extend the above model to the regime of arbitrary excitation energies, we split the energy space above $E_{i,th}$ into zones with a width defined by the energy lost in an individual CM event (E_{loss}; Figure 3a). Then, we calculate QE from $\eta = \sum_{i=e,h}\sum_{j=0,m-1}(jP^i_{m,j})$, where $P^i_{m,j}$ is the probability of generating j additional excitons if the carrier was originally introduced into zone m; for a given excitation energy E_i, m can be calculated from $m = \lfloor(E_i - E_{i,th})/E_{loss}\rfloor + 1$ and j is from 0 to $(m - 1)$.

Independent of excitation energy, we can describe the probability of *not* having CM as $P^i_0 = \exp[-(E_i - E_{i,th})/\varepsilon_{eh}]$.

dx.doi.org/10.1021/jz4004334 | J. Phys. Chem. Lett. 2013, 4, 2061−2068

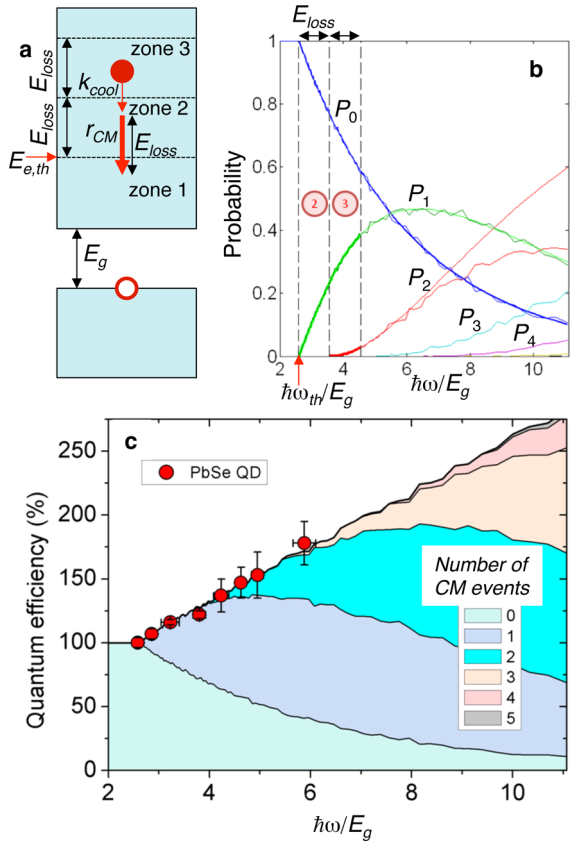

Figure 3. Phenomenological model of CM. (a) A hot carrier dissipates energy by either undergoing a CM event (E_{loss} is energy loss per event; characteristic rate $r_{CM} = 1/\tau_{CM}$) or a non-CM energy relaxation pathway due, for example, to phonon emission (k_{cool} is a corresponding energy loss rate). E_{loss} defines the size of the zone with a different number of possible CM events; CM is not possible in zone 1, one CM event is possible in zone 2, two in zone 3, and so forth. (b) In each zone, we calculate the probability for zero (P_0; blue), one (P_1; green), two (P_2; red), and so forth CM events to occur. The results of analytical calculations are shown by smooth lines (used in zones 1−3 and account for no more than two additional excitons). The results of numerical Monte Carlo calculations are shown by jagged lines; these results are in good agreement with analytical calculations up to excitation energies for which the probability of generating three additional excitons becomes significant. (c) The QE of CM is the sum of weighted probabilities accounting for a different number of CM events in a given zone. The Monte Carlo model (solid jagged lines) is used to fit the measured QEs for PbSe QDs (circles) and to extract the e−h pair creation energy. The shaded filling indicates how the QE is composed of different types of CM events (that is, zero, one, two, etc. additional excitons produced via CM).

This expression can be obtained by splitting the entire relaxation window T into small segments Δt ($\Delta t \ll \tau_{CM}$). In each segment, the probability of not having CM is $(1 - \Delta t/\tau_{CM})$. By multiplying probabilities for all segments within T, we obtain $(1 - \Delta t/\tau_{CM})^{(T/\Delta t)}$, which converges to $\exp(-T/\tau_{CM})$ or $\exp[-(E_i - E_{i,th})/(\tau_{CM}k_{cool})]$ in the limit $\Delta t \to 0$; here, we use $T = (E_i - E_{i,th})/k_{cool}$.

Using probability P^i_0, we can easily obtain $P^i_{1,1}$ for zone 2, where only one additional exciton can be generated, and hence, $P^i_{2,1} = 1 - P^i_0 = 1 - \exp[-(E_i - E_{i,th})/(\tau_{CM}k_{cool})]$. For small excess energies when $(E_i - E_{i,th}) \ll \tau_{CM}k_{cool}$, $\eta_i = P^i_{2,1} \approx (E_i - E_{i,th})/(\tau_{CM}k_{cool})$, which yields $\varepsilon_{eh} = dE_i/d\eta_i = \tau_{CM}k_{cool}$, in agreement with the earlier estimation. Via more involved calculations, we obtain for zone 3 $P^i_{3,1} = [1 + (E_i - E_{i,th} - E_{loss})/\varepsilon_{eh} - \exp(-E_{loss}/\varepsilon_{eh})]\exp[-(E_i - E_{i,th} - E_{loss})/\varepsilon_{eh}]$ and $P^i_{3,2} = 1 - P^i_{2,0} - P^i_{2,1}$.

Because of the complexity of analytic calculations for zone 4 and higher, we complement them with a Monte Carlo analysis. Briefly, in our numerical simulations, we break down the relaxation time window T into small segments Δt and propagate a carrier downward in energy from segment to segment assuming that at each relaxation step, it can undergo CM with a probability $\Delta t/\tau_{CM}$. If a CM event is registered, E_{loss}/k_{cool} worth of time is removed from the array, reducing the time window in which remaining CM events may occur. This process is repeated many times for each T to establish the distribution of probabilities for different numbers of CM events. The multiexciton yield is determined by summing the probabilities multiplied by the corresponding numbers of additional e−h pairs produced via CM.

In Figure 3b, we compare the results of Monte Carlo calculations (jagged lines) with those of the analytical model (smooth lines). Both calculations are in good agreement up to $\hbar\omega/E_g$ of ∼6. At higher excitation energies, when the probability of generating three additional excitons becomes significant, we observe the expected deviation between the two types of calculations.

In Figure 3c, we present the analysis of QEs for PbSe QDs (the same data set as that in Figure 2c) using the above model. Previous studies of the E_g dependence of Auger recombination in PbSe QDs strongly suggest that momentum conservation in these structures is relaxed, at least in the case of multicarrier processes.[6] Therefore, in our modeling, we neglect the "kinetic" contribution to ε_{eh} resulting from momentum conservation[52] and assume that E_{loss} is defined solely by energy conservation, that is, $E_{loss} = E_g$.

Our next assumption relates to the distribution of the photon energy in excess of E_g between the electron and the hole. In the case of strict parity conservation, optical transitions can only couple valence and conduction band states of the same symmetry (that is, $1S_h$ to $1S_e$, $1P_h$ to $1P_e$, etc.). Further, as electron and hole masses in Pb chalcogenides are almost identical, the optical transitions are expected to produce conduction and valence band carriers with equal energies ($E_e = E_h$). Combined with energy conservation, this seems to suggest that in Pb chalcogenide QDs, the CM threshold is at least $3E_g$ (obtained from $\hbar\omega_{th} = E_g + E_{e,th} + E_{h,th}$ and $E_{e,th} = E_{h,th} = E_g$). However, the measurements of the present work as well as those of earlier reports[30,47] indicate that the CM threshold in these QDs is appreciably lower than $3E_g$, implying that the energy of one of the carriers produced by photoexcitation can be significantly higher than that of the other carrier. The possible reasons for this uneven distribution of energy between the electron and hole may include the contribution from asymmetric transitions resulting from, for example, band anisotropies[53,54] and/or relaxation of parity conservation[55,56] or, perhaps, quick energy redistribution between the electron and the hole due to very fast (subpicosecond) e−h scattering.[57] On the basis of the above considerations, we assume, for simplicity, that the excess photon energy is entirely transferred to one carrier (e.g., an electron) and further use the experimentally measured CM spectroscopic threshold of $\sim 2.7E_g$.

These assumptions leave us with just one adjustable parameter: ε_{eh}. To model the data in Figure 3, where E_g is tuned through quantum confinement (that is, by QD size), we

dx.doi.org/10.1021/jz4004334 | J. Phys. Chem. Lett. 2013, 4, 2061−2068

allow ε_{eh} to vary as a function of confinement energy E_c. We find that the experimental results are best described when ε_{eh} scales linearly with E_c, suggesting the existence of a direct relationship between the e−h pair creation energy and the band gap energy. Interestingly, the studies of bulk semiconductors also indicate a direct linear scaling of ε_{eh} with E_g. For example, in wide-gap semiconductors, ε_{eh} is $\sim 3E_g$,[52] while the numerical prefactor increases to 5−7 in narrow-gap PbS and PbSe.[58,59]

While being somewhat suggestive, the observations made for bulk solids may not necessarily apply to QDs. In fact, the direct dependence of ε_{eh} on E_c in this case likely emerges as a result of an interplay between size dependences of k_{cool} and τ_{CM}. Specifically, it is well-known (Figure 2a and refs 48 and 60) that Auger lifetimes in QDs scale as R^3 (R is the QD radius) and hence approximately as $(E_c)^{-3/2}$ if we assume that $E_c \propto 1/R^2$. On the other hand, previous measurements of 1P−1S intraband cooling in PbSe QDs indicate that the corresponding energy loss rate (k_{1P1S}) scales approximately as $(E_c)^{5/2}$.[61] If these quantities are used as proxies for, respectively, τ_{CM} and k_{cool}, we find that ε_{eh} indeed scales as E_c or directly as E_g in the limit of strong quantization, which corresponds to large confinement energies.

By applying our model to all three types of QD samples (jagged lines in Figure 2c), we find relative ratios of ε_{eh} to be 1:1.8:4.5 for PbTe, PbSe, and PbS QDs, which is in agreement with the ratios (1:1.5:4.5) derived from linear fits to the measured QEs (not shown). Given the expected similarity of τ_{CM} values in these materials, the observed differences in ε_{eh} should be ascribed to the difference in non-CM relaxation rates.

To evaluate the non-CM intraband energy loss rate, we analyze band edge 1S state-filling dynamics.[57,61] We acknowledge that the energy loss rate measured in this way may differ from that at higher energies that are more relevant to the CM process. However, we speculate that it can still be used as a surrogate for τ_{CM} in the comparison between QDs of different compositions as it is unlikely that the composition-dependent trends at high carrier energies are different from those at lower energies. Specifically, even if the dominant channel for non-CM energy losses changes from single-phonon emission (expected for relaxation within the dense spectrum of bulk-like, high-energy states) to multiphonon emission[61] (which might be involved at near-band-edge energies), both of these processes are still described by the same matrix elements of the carrier−phonon interaction and, therefore, should exhibit similar composition-dependent trends from one QD sample to the other.

In Figure 4, we compare the 1S population buildup measured by TA for QDs of all three compounds with matching band gaps of ∼0.86 eV. We identify two contributions to the measured traces. The earliest and fastest rise (red circles) we associate with a Coulomb shift due to the interaction of the band edge 1S exciton with a high-energy exciton created by the pump pulse.[2,57,62] This is followed by a slower rise (black circles), which we attribute to 1S state filling.[57] Fitting this slower rise to a single exponential (red curve), we extract a time constant (τ_{1P1S}), which we use to calculate k_{1P1S} from $k_{1P1S} = \Delta E_{1P1S}/\tau_{1P1S}$, where ΔE_{1P1S} is the energy dissipated between the 1P and 1S states (which are indicated by arrows in the insets of Figure 4).

In this way, we estimate the cooling rates to be k_{1P1S}(PbTe):k_{1P1S}(PbSe):k_{1P1S}(PbS) ≈ 1:2.0:4.2. These results are in excellent correspondence with the ratios among the e−h pair creation energies derived from the modeling, confirming

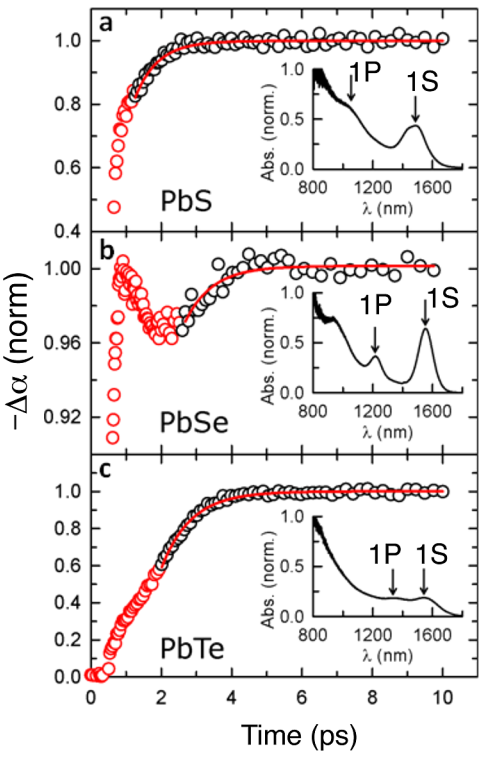

Figure 4. Measurements of non-CM intraband relaxation. We gain information on the relative values of non-CM energy loss rates from characteristic times of 1P-to-1S relaxation (derived from fits shown by red lines) measured using a TA experiment (open circles) with a probe wavelength tuned in resonance with the lowest-energy 1S absorption feature (PbS in (a), PbSe in (b), and PbTe in (c)); the band gap of all samples is ∼0.86 eV. Using linear absorption spectra (insets), we determine the energy difference between the 1P and the 1S states used in the calculations of the energy loss rate. These data indicate that the energy dissipation rate near the band edge in PbTe QDs is lower than that in PbSe QDs, which in turn is lower than that in PbS QDs.

that the observed differences in ε_{eh} and the CM yields between PbTe, PbSe, and PbS QDs are primarily due to the difference in non-CM relaxation rates. While the measured band edge rates might be different from absolute values of k_{cool} at higher more-CM-relevant energies, it is unlikely that the material's specific trends in intraband relaxation are dependent on the exact energy of the relaxing carrier. Therefore, a comparison of CM-relevant cooling rates between different compositions should be possible using the near-band-edge relaxation data.

A very suggestive corroboration for our measured rates of carrier cooling can be made by analyzing energy loss rates in bulk forms of the three materials studied in this work. Carrier cooling in Pb chalcogenides is dominated by polar coupling to longitudinal optical (LO) phonons. The corresponding energy loss rate can be estimated from $k_{cool,0} \propto \alpha_{pol}\hbar\omega_{LO}$, where α_{pol} is the polar coupling constant, the subscript naught indicates a bulk parameter, and $\hbar\omega_{LO}$ is the LO phonon energy.[63] Using literature data for α_{pol} and $\hbar\omega_{LO}$,[64] we estimate that $k_{cool,0}$(PbTe):$k_{cool,0}$(PbSe):$k_{cool,0}$(PbS) = 1:2.9:7.4, which demonstrates the same trend as that revealed by direct measurement of the k_{1P1S} rates for the QDs. This suggests that perhaps a preliminary evaluation of k_{loss} in QDs can be conducted on the basis of relaxation parameters of parental bulk solids.

Recent studies of elongated nanocrystals, or nanorods (NRs), suggest that one promising approach to enhancing CM efficiency is through shape control, which might allow one

dx.doi.org/10.1021/jz4004334 | J. Phys. Chem. Lett. 2013, 4, 2061−2068

to manipulate τ_{CM} by manipulating the strength of carrier−carrier Coulomb coupling.[24,25] The first report on CM in PbSe NRs[26] suggested a very significant increase of QEs compared to spherically shaped QDs, with both $\varepsilon_{eh} \approx 1.2E_g$ and $\hbar\omega_{CM} \approx 2.2E_g$ approaching the respective energy-conservation-defined limits (E_g and $2E_g$, respectively). More recent studies of the effect of nanocrystal elongation on CM[24,25] also indicate an enhancement of QE in PbSe NRs but less substantial than those in ref 26. These newer measurements also show that CM yields depend on the NR aspect ratio, ρ (the ratio of the rod length to its diameter), and exhibit a maximum at ρ = 6−7 when the CM-enhancement in NRs versus QDs reaches a value of about 2 (evaluated in terms of the multiexciton yield).[25] The measured CM threshold in NRs ($\hbar\omega_{th} \approx 2.6E_g$) is close to that in QDs ($\hbar\omega_{th} \approx 2.7E_g$), suggesting that the observed enhancement in QE is primarily due to a decrease in the e−h pair creation energy. On the basis of the QEs measured for NRs with the optimal aspect ratio, ε_{eh} is $2.7E_g$ versus the size average ε_{eh} of $4.3E_g$ in PbSe QDs (Figure 2c).

One intriguing outcome of the measurements of PbSe NRs is the somewhat unexpected observation of opposite trends in CM and Auger recombination efficiencies upon nanocrystal elongation. On the basis of recent studies of PbSe QDs and NRs, both of these structures are characterized by similar intraband dynamics[65] (that is, similar k_{cool}), suggesting that the CM enhancement observed in NRs with moderate elongation is likely a result of a shortening of τ_{CM}. This would seem to also suggest shortening of Auger lifetimes. However, the τ_{2A} constants for NRs are systematically longer than those for the QDs.[25] To explain this apparent discrepancy, one can invoke the difference in the character of high- and low-energy excitations in the NRs. Indeed, due to strong e−h attraction typical in one-dimensional (1D) semiconductors, band edge electrons and holes in the NRs bind into tightly confined excitons.[66,67] As a result, Auger recombination becomes less efficient than that in QDs as it occurs via two-particle collisions of weakly interacting charge-neutral excitons.[66,68,69] The situation, however, is different in the case of CM, which involves hot, unrelaxed charges before they form bound excitonic states. In this way, the CM mechanism in NRs is likely similar to that in QDs, but it is mediated by a stronger Coulomb interaction, which is enhanced due to reduced dielectric screening and the 1D character of electronic states.[66,67]

To summarize, the data and analysis presented here strongly suggest that the efficiency of CM is set by the competition of two relaxation pathways: impact-ionization-like scattering and non-CM relaxation due, for example, to phonon emission. This analysis allows one to more predictably search for materials with greater CM efficiencies based on parameters of parental bulk solids. An important implication is that simple monocomponent QDs may not be sufficient to obtain large enhancements in the CM efficiency. Indeed, it is well established that QD volume (V), *not* QD composition, appears to be the determining factor in Auger recombination.[48,60] This suggests that the CM rates are likely to behave in a similarly universal V-dependent fashion, independent of composition. On the other hand, the remaining means for control, namely, through the phonon emission rate, does not appear to have significant room for improvement over PbTe, although materials such as InSb and InAs do have slightly more favorable polar coupling constants. These arguments suggest a need for nanoengineered structures specifically designed to slow down hot carrier relaxation and/or enhance CM rates.

These arguments suggest a need for nanoengineered structures specifically designed to slow down hot carrier relaxation and/or enhance CM rates.

Recent studies of PbSe NRs suggest that shape control is a promising approach for enhancing CM efficiency. Specifically, using NRs with an optimal aspect ratio of 6−7, one can obtain an approximately 2-fold increase in the multiexciton yield, which comes primarily from a reduction in the e−h pair creation energy.[24,25] A promising next step in studies of elongated structures would be measurements of PbTe NRs that might show even greater CM enhancement due to reduced electron−phonon coupling.

Another interesting direction is the study of heterostructured nanocrystals that should allow for even greater flexibility in controlling Coulomb interactions, carrier dynamics, and the band gap energy compared to monocomponent QDs or NRs. Hybrid structures combining semiconductor nanocrystals with nanoscale metals[70] are also of interest due to a potential effect of surface plasmons on both electron−photon and electron−electron interactions. An important instrumental direction is the development of novel tools for quick and reliable screening of CM in infrared nanostructures, which would facilitate the search for new more efficient CM materials. One promising technique is based on high-sensitivity, time-resolved measurements with a superconducting single-photon detector.[24] However, there is still a significant need for simpler methods that would rely not on complex time-resolved experiments but rather on spectroscopic steady-state measurements.

AUTHOR INFORMATION

Corresponding Author

*E-mail klimov@lanl.gov.

Notes

The authors declare no competing financial interest.

Biographies

John T. Stewart (http://quantumdot.lanl.gov/stewart.shtml) is a Director's Postdoctoral Fellow in the Nanotechnology and Advanced Spectroscopy (NanoTech) team, Chemistry Division, Los Alamos National Laboratory (LANL). He received B.S. degrees in Physics and Mathematics from Texas A&M University (2004) and a Ph.D. in Physics from the University of Colorado, Boulder (2009). His research centers on probing novel light−matter interactions.

Lazaro A. Padilha (http://quantumdot.lanl.gov/padilha.shtml) is a Postdoctoral Research Associate in the NanoTech Team. He received his B.Sc. (2001) and Ph.D. (2006) in Physics from the State University of Campinas, Brazil. His research focuses on light−matter interactions in nanostructures

Wan Ki Bae (http://quantumdot.lanl.gov/bae.shtml) is a Postdoctoral Research Associate in the NanoTech team. He received his B.S. (2003), M.S. (2005), and Ph.D. (2009) in Chemical Engineering from Seoul National University, South Korea. His research interests include synthesis and device applications of colloidal nanostructures.

Weon-kyu Koh (http://quantumdot.lanl.gov/koh.shtml) is a Postdoctoral Research Associate in the NanoTech team. He received his B.S. (2000) and M.S. (2002) in Chemistry from Seoul National University, South Korea, and a Ph.D. in Inorganic Chemistry from the University of Pennsylvania (2011). His current research interests include synthesis and charge-transport properties of colloidal nanocrystals.

Jeffrey M. Pietryga (http://quantumdot.lanl.gov/pietryga.shtml) is a Technical Staff Member in the NanoTech team. He received a B.S. in Chemistry from the University of Michigan-Flint (1997) and a Ph.D. in Inorganic Chemistry from the University of Texas, Austin (2002). His current research centers on synthesis and characterization of new infrared-active nanocrystal materials.

Victor I. Klimov (http://quantumdot.lanl.gov/klimov.shtml) is a LANL Fellow, the director of the Center for Advanced Solar Photophysics, and the leader of the NanoTech team. He received his M.S. (1978), Ph.D. (1981), and D.Sc. (1993) degrees from Moscow State University, Russia. His current research interests include photophysics of semiconductor and metal nanostructures and their applications in solar energy conversion.

■ ACKNOWLEDGMENTS

We acknowledge support of the Center for Advanced Solar Photophysics (CASP), an Energy Frontier Research Center funded by the U.S. Department of Energy, Office of Science, Office of Basic Energy Sciences.

■ REFERENCES

(1) Brendel, R.; Werner, J. H.; Queisser, H. J. Thermodynamic Efficiency Limits for Semiconductor Solar Cells with Carrier Multiplication. *Sol. Energy Mater. Sol. Cells* **1996**, *41/42*, 419−425.
(2) Klimov, V. I. Spectral and Dynamical Properties of Multilexcitons in Semiconductor Nanocrystals. *Annu. Rev. Phys. Chem.* **2007**, *58*, 635−673.
(3) Kambhampati, P. Multiexcitons in Semiconductor Nanocrystals: A Platform for Optoelectronics at High Carrier Concentration. *J. Phys. Chem. Lett* **2012**, *3*, 1182−1190.
(4) Landsberg, P. T. *Recombination in Semiconductors*; University Press: Cambridge, U.K., 1991.
(5) Nozik, A. J. Quantum Dot Solar Cells. *Physica E* **2002**, *14*, 115−120.
(6) Pietryga, J. M.; Zhuravlev, K. K.; Whitehead, M.; Klimov, V. I.; Schaller, R. D. Evidence for Barrierless Auger Recombination in PbSe Nanocrystals: A Pressure-Dependent Study of Transient Optical Absorption. *Phys. Rev. Lett.* **2008**, *101*, 217401.
(7) Schaller, R. D.; Klimov, V. I. High Efficiency Carrier Multiplication in PbSe Nanocrystals: Implications for Solar Energy Conversion. *Phys. Rev. Lett.* **2004**, *92*, 186601.
(8) Ellingson, R. J.; Beard, M. C.; Johnson, J. C.; Yu, P. R.; Micic, O. I.; Nozik, A. J.; Shabaev, A.; Efros, A. L. Highly Efficient Multiple Exciton Generation in Colloidal PbSe and PbS Quantum Dots. *Nano Lett.* **2005**, *5*, 865−871.
(9) Trinh, M. T.; Houtepen, A. J.; Schins, J. M.; Hanrath, T.; Piris, J.; Knulst, W.; Goossens, A. P. L. M.; Siebbeles, L. D. A. In Spite of Recent Doubts Carrier Multiplication Does Occur in PbSe Nanocrystals. *Nano Lett.* **2008**, *8*, 1713−1718.
(10) Nair, G.; Geyer, S. M.; Chang, L.-Y.; Bawendi, M. G. Carrier Multiplication Yields in PbS and PbSe Nanocrystals Measured by Transient Photoluminescence. *Phys. Rev. B* **2008**, *78*, 125325−1−10.
(11) Ji, M.; Park, S.; Connor, S. T.; Mokari, T.; Cui, Y.; Gaffney, K. J. Efficient Multiple Exciton Generation Observed in Colloidal PbSe Quantum Dots with Temporally and Spectrally Resolved Intraband Excitation. *Nano Lett.* **2009**, *9*, 1217−1222.
(12) Gesuele, F.; Sfeir, M. Y.; Koh, W. K.; Murray, C. B.; Heinz, T. F.; Wong, C. W. Ultrafast Supercontinuum Spectroscopy of Carrier Multiplication and Biexcitonic Effects in Excited States of PbS Quantum Dots. *Nano Lett.* **2012**, *12*, 2658−2664.
(13) Beard, M. C. Multiple Exciton Generation in Semiconductor Quantum Dots. *J. Phys. Chem. Lett.* **2011**, *2*, 1282−1288.
(14) Stubbs, S. K.; Hardman, S. J. O.; Graham, D. M.; Spencer, B. F.; Flavell, W. R.; Glarvey, P.; Masala, O.; Pickett, N. L.; Binks, D. J. Efficient Carrier Multiplication in InP Nanoparticles. *Phys. Rev. B* **2010**, 81.
(15) Xiao, J.; Wang, Y.; Hua, Z.; Wang, X.; Zhang, C.; Xiao, M. Carrier Multiplication in Semiconductor Nanocrystals Detected by Energy Transfer to Organic Dye Molecules. *Nat. Commun.* **2012**, 3.
(16) Yang, Y.; Rodriguez-Cordoba, W.; Lian, T. Q. Multiple Exciton Generation and Dissociation in PbS Quantum Dot−Electron Acceptor Complexes. *Nano Lett.* **2012**, *12*, 4235−4241.
(17) Zhu, H. M.; Lian, T. Q. Enhanced Multiple Exciton Dissociation from CdSe Quantum Rods: The Effect of Nanocrystal Shape. *J. Am. Chem. Soc.* **2012**, *134*, 11289−11297.
(18) Sukhovatkin, V.; Hinds, S.; Brzozowski, L.; Sargent, E. H. Colloidal Quantum-Dot Photodetectors Exploiting Multiexciton Generation. *Science* **2009**, *324*, 1542−1544.
(19) Sambur, J. B.; Novet, T.; Parkinson, B. A. Multiple Exciton Collection in a Sensitized Photovoltaic System. *Science* **2010**, *330*, 63−66.
(20) Semonin, O. E.; Luther, J. M.; Chen, S. C. H.-Y.; Gao, J.; Nozik, A. J.; Beard, M. C. Peak External Photocurrent Quantum Efficiency Exceeding 100% via MEG in a Quantum Dot Solar Cell. *Science* **2011**, 1530−1533.
(21) Hanna, M. C.; Nozik, A. J. Solar Conversion Efficiency of Photovoltaic and Photoelectrolysis Cells with Carrier Multiplication Absorbers. *J. Appl. Phys.* **2006**, *100*, 074510/1−074510/8.
(22) Klimov, V. I. Detailed-Balance Power Conversion Limits of Nanocrystal-Quantum-Dot Solar Cells in the Presence of Carrier Multiplication. *Appl. Phys. Lett.* **2006**, *89*, 123118/1−123118/3.
(23) Hanna, M. C.; Beard, M. C.; Nozik, A. J. Effect of Solar Concentration on the Thermodynamic Power Conversion Efficiency of Quantum-Dot Solar Cells Exhibiting Multiple Exciton Generation. *J. Phys. Chem. Lett.* **2012**, *3*, 2857−2862.
(24) Sandberg, R. L.; Padilha, L. A.; Qazilbash, M. M.; Bae, W. K.; Schaller, R. D.; Pietryga, J. M.; Stevens, M. J.; Baek, B.; Nam, S. W.; Klimov, V. I. Multiexciton Dynamics in Infrared-Emitting Colloidal Nanostructures Probed by a Superconducting Nanowire Single-Photon Detector. *ACS Nano* **2012**, *6*, 9532−9540.
(25) Padilha, L. A.; Stewart, J. T.; Sandberg, R. L.; Bae, W. K.; Koh, E.-k.; Pietryga, J. M.; Klimov, V. I. Aspect Ratio Dependence of Auger Recombination and Carrier Multiplication in PbSe Nanorods. *Nano Lett.* **2013**, *13*, 1092−1099.
(26) Cunningham, P. D.; Boercker, J. E.; Foos, E. E.; Lumb, M. P.; Smith, A. R.; Tischler, J. G.; Melinger, J. S. Enhanced Multiple Exciton Generation in Quasi-One-Dimensional Semiconductors. *Nano Lett.* **2011**, *11*, 3476−3481.
(27) Beard, M. C.; Knutsen, K. P.; Yu, P.; Luther, J. M.; Song, Q.; Metzger, W. K.; Ellingson, R. J.; Nozik, A. J. Multiple Exciton Generation in Colloidal Silicon Nanocrystals. *Nano Lett.* **2007**, *7*, 2506−2512.
(28) Timmerman, D.; Valenta, J.; Dohnalova, K.; de Boer, W. D. A. M.; Gregorkiewicz, T. Step-like Enhancement of Luminescence Quantum Yield of Silicon Nanocrystals. *Nat. Nanotechnol.* **2011**, *6*, 710−713.
(29) Trinh, M. T.; Limpens, R.; de Boer, W. D. A. M.; Schins, J. M.; Siebbeles, L. D. A.; Gregorkiewicz, T. Direct Generation of Multiple Excitons in Adjacent Silicon Nanocrystals Revealed by Induced Absorption. *Nat. Photonics* **2012**, *6*, 316−321.
(30) Beard, M. C.; Midgett, A. G.; Hanna, M. C.; Luther, J. M.; Hughes, B. K.; Nozik, A. J. Comparing Multiple Exciton Generation in Quantum Dots to Impact Ionization in Bulk Semiconductors: Implications for Enhancement of Solar Energy Conversion. *Nano Lett.* **2010**, *10*, 3019−3027.

(31) Califano, M. Photoinduced Surface Trapping and the Observed Carrier Multiplication Yields in Static CdSe Nanocrystal Samples. *ACS Nano* **2011**, *5*, 3614−3621.
(32) Califano, M.; Zunger, A.; Franceschetti, A. Efficient Inverse Auger Recombination at Threshold in CdSe Nanocrystals. *Nano Lett.* **2004**, *4*, 525−531.
(33) Franceschetti, A.; An, J. M.; Zunger, A. Impact Ionization Can Explain Carrier Multiplication in PbSe Quantum Dots. *Nano Lett.* **2006**, *6*, 2191−2195.
(34) Allan, G.; Delerue, C. Role of Impact Ionization in Multiple Exciton Generation in PbSe Nanocrystals. *Phys. Rev. B* **2006**, *73*, 205423.
(35) Rabani, E.; Baer, R. Theory of Multiexciton Generation in Semiconductor Nanocrystals. *Chem. Phys. Lett.* **2010**, *496*, 227−235.
(36) Baer, R.; Rabani, E. Expeditious Stochastic Calculation of Multiexciton Generation Rates in Semiconductor Nanocrystals. *Nano Lett.* **2012**, *12*, 2123−2128.
(37) Shabaev, A.; Efros, A. L.; Nozik, A. J. Multiexciton Generation by a Single Photon in Nanocrystals. *Nano Lett.* **2006**, *6*, 2856−2863.
(38) Witzel, W. M.; Shabaev, A.; Hellberg, C. S.; Jacobs, V. L.; Efros, A. L. Quantum Simulation of Multiple-Exciton Generation in a Nanocrystal by a Single Photon. *Phys. Rev. Lett.* **2010**, 105.
(39) Prezhdo, O. V. Multiple Excitons and the Electron−Phonon Bottleneck in Semiconductor Quantum Dots: An Ab Initio Perspective. *Chem. Phys. Lett.* **2008**, *460*, 1−9.
(40) Schaller, R. D.; Agranovich, V. M.; Klimov, V. I. High-Efficiency Carrier Multiplication through Direct Photogeneration of Multi-Excitons via Virtual Single-Exciton States. *Nat. Phys.* **2005**, *1*, 189−194.
(41) Rupasov, V. I.; Klimov, V. I. Carrier Multiplication in Semiconductor Nanocrystals via Intraband Optical Transitions Involving Virtual Biexciton States. *Phys. Rev. B* **2007**, *76*, 125321.
(42) Hyeon-Deuk, K.; Prezhdo, O. V. Photoexcited Electron and Hole Dynamics in Semiconductor Quantum Dots: Phonon-Induced Relaxation, Dephasing, Multiple Exciton Generation and Recombination. *J. Phys.: Condens. Matter* **2012**, 24.
(43) Hyeon-Deuk, K.; Prezhdo, O. V. Multiple Exciton Generation and Recombination Dynamics in Small Si and CdSe Quantum Dots: An Ab Initio Time-Domain Study. *ACS Nano* **2012**, *6*, 1239−1250.
(44) Timmerman, D.; Izeddin, I.; Stallinga, P.; Yassievich, I. N.; Gregorkiewicz, T. Space-Separated Quantum Cutting with Silicon Nanocrystals for Photovoltaic Applications. *Nat. Photonics* **2008**, *2*, 105−109.
(45) Govoni, M.; Marri, I.; Ossicini, S. Carrier Multiplication between Interacting Nanocrystals for Fostering Silicon-Based Photovoltaics. *Nat. Photonics* **2012**, *6*, 672−679.
(46) Stewart, J. T.; Padilha, L. A.; Qazilbash, M. M.; Pietryga, J. M.; Midgett, A. G.; Luther, J. M.; Beard, M. C.; Nozik, A. J.; Klimov, V. I. Comparison of Carrier Multiplication Yields in PbS and PbSe Nanocrystals: The Role of Competing Energy-Loss Processes. *Nano Lett.* **2012**, *12*, 622−628.
(47) McGuire, J. A.; Joo, J.; Pietryga, J. M.; Schaller, R. D.; Klimov, V. I. New Aspects of Carrier Multiplication in Semiconductor Nanocrystals. *Acc. Chem. Res.* **2008**, *41*, 1810−1819.
(48) Klimov, V. I.; Mikhailovsky, A. A.; McBranch, D. W.; Leatherdale, C. A.; Bawendi, M. G. Quantization of Multiparticle Auger Rates in Semiconductor Quantum Dots. *Science* **2000**, *287*, 1011−1013.
(49) McGuire, J. A.; Sykora, M.; Joo, J.; Pietryga, J. M.; Klimov, V. I. Apparent versus True Carrier Multiplication Yields in Semiconductor Nanocrystals. *Nano Lett.* **2010**, *10*, 2049−2057.
(50) McGuire, J. A.; Sykora, M.; Robel, I.; Padilha, L. A.; Joo, J.; Pietryga, J. M.; Klimov, V. I. Spectroscopic Signatures of Photocharging due to Hot-Carrier Transfer in Solutions of Semiconductor Nanocrystals under Low-Intensity Ultraviolet Excitation. *ACS Nano* **2010**, *4*, 6087−6097.
(51) Padilha, L. A.; Robel, I.; Lee, D. C.; Nagpal, P.; Pietryga, J. M.; Klimov, V. I. Spectral Dependence of Nanocrystal Photoionization Probability: The Role of Hot-Carrier Transfer. *ACS Nano* **2011**, *5*, 5045−5055.
(52) Alig, R. C.; Bloom, S. Electron−Hole-Pair Creation Energy in Semiconductors. *Phys. Rev. Lett.* **1975**, *35*, 1522−1525.
(53) An, J. M.; Franceschetti, A.; Dudiy, S. V.; Zunger, A. The Peculiar Electronic Structure of PbSe Quantum Dots. *Nano Lett.* **2006**, *6*, 2728−2735.
(54) Tudury, G. E.; Marquezini, M. V.; Ferreira, L. G.; Barbosa, L. C.; Cesar, C. L. Effect of Band Anisotropy on Electronic Structure of PbS, PbSe, and PbTe Quantum Dots. *Phys. Rev. B* **2000**, *62*, 7357−7364.
(55) Goupalov, S. V. Selection Rules for Optical Transitions in PbSe Nanocrystal Quantum Dots: Drastic Effect of Structure Inversion Asymmetry. *Phys. Rev. B* **2009**, *79*, 233305.
(56) Diaconescu, B.; Padilha, L. A.; Nagpal, P.; Swartzentruber, B. S.; Klimov, V. I. Measurement of Electronic States in PbS Nanocrystal Quantum Dots Using Scanning Tunneling Spectroscopy: The Role of Parity Selection Rules in Optical Absorption. *Phys. Rev. Lett.* **2013**, *110*, 127406.
(57) Klimov, V. I.; McBranch, D. W. Femtosecond 1P-to-1S Electron Relaxation in Strongly-Confined Semiconductor Nanocrystals. *Phys. Rev. Lett.* **1998**, *80*, 4028−4031.
(58) Smith, A.; Dutton, D. Behavior of Lead Sulfide Photocells in the Ultraviolet. *J. Opt. Soc. Am.* **1958**, *48*, 1007−1009.
(59) Pijpers, J. J. H.; Ulbricht, R.; Tielrooij, K. J.; Osherov, A.; Golan, Y.; Delerue, C.; Allan, G.; Bonn, M. Assessment of Carrier-Multiplication Efficiency in Bulk PbSe and PbS. *Nat. Phys.* **2009**, *5*, 811−814.
(60) Robel, I.; Gresback, R.; Kortshagen, U.; Schaller, R. D.; Klimov, V. I. Universal Size-Dependent Trend in Auger Recombination in Direct-Gap and Indirect-Gap Semiconductor Nanocrystals. *Phys. Rev. Lett.* **2009**, *102*, 177404.
(61) Schaller, R. D.; Pietryga, J. M.; Goupalov, S. V.; Petruska, M. A.; Ivanov, S. A.; Klimov, V. I. Breaking the Phonon Bottleneck in Semiconductor Nanocrystals via Multiphonon Emission Induced by Intrinsic Nonadiabatic Interactions. *Phys. Rev. Lett.* **2005**, *95*, 196401/1−196401/4.
(62) Klimov, V.; Hunsche, S.; Kurz, H. Biexciton Effects in Femtosecond Nonlinear Transmission of Semiconductor Quantum Dots. *Phys. Rev. B* **1994**, *50*, 8110−8113.
(63) Ridley, B. K. *Quantum Processes in Semiconductors*; Oxford University Press Inc.: Oxford, U.K., 1999.
(64) *Non-Tetrahedrally Bonded Elements and Binary Compounds*, New Series, Group III ed.; Madelung, O., Schulz, M., Weiss, H., Eds.; Springer: Berlin, Germany, 1998.
(65) Yang, J.; Hyun, B. R.; Basile, A. J.; Wise, F. W. Exciton Relaxation in PbSe Nanorods. *ACS Nano* **2012**, *6*, 8120−8127.
(66) Wang, F.; Wu, Y.; Hybertsen, M. S.; Heinz, T. F. Auger Recombination of Excitons in One-Dimensional Systems. *Phys. Rev. B* **2006**, *73*, 245424.
(67) Bartnik, A. C.; Efros, A. L.; Koh, W. K.; Murray, C. B.; Wise, F. W. Electronic States and Optical Properties of PbSe Nanorods and Nanowires. *Phys. Rev. B* **2010**, *82*, 195313.
(68) Achermann, M.; Bartko, A. P.; Hollingsworth, J. A.; Klimov, V. I. The Effect of Auger Heating on Intraband Carrier Relaxation in Semiconductor Qauntum Dots. *Nat. Phys.* **2006**, *2*, 557−561.
(69) Htoon, H.; Hollingsworth, J. A.; Dickerson, R.; Klimov, V. I. Zero- to One-Dimensional Transition and Auger Recombination in Semiconductor Quantum Rods. *Phys. Rev. Lett.* **2003**, *91*, 227401/1−227401/4.
(70) Khanal, B. P.; Pandey, A.; Li, L.; Bae, W. K.; Klimov, V. I.; Pietryga, J. M. Generalized Synthesis of Hybrid Metal−Semiconductor Nanostructures Tunable from the Visible to the Infrared. *ACS Nano* **2011**, *6*, 3832−3840.